Q. J. R. Meteorol. Soc. (2000), **126**, pp. 145–171

Stability properties of and scaling laws for a dry radiative–convective atmosphere

By VINCENT E. LARSON*
Massachusetts Institute of Technology, USA

(Received 8 December 1998; revised 17 June 1999)

SUMMARY

This work is a theoretical and numerical study of the stability properties and scaling laws associated with an idealized radiative–convective model. We find that the linear-stability threshold in the model can be described by a radiative Rayleigh number, a parameter that incorporates radiative effects but otherwise resembles the classical Rayleigh number. The energy method is used to find a nonlinear-stability threshold below which all perturbations, whether infinitesimal or finite-amplitude, decay. The model behaviour when weakly nonlinear convection occurs is studied via the mean-field equations. We find that changing the values of viscosity, thermal diffusivity, and radiative damping has only weak effects on the vertical convective heat flux, in contrast to the case for weakly nonlinear Rayleigh–Bénard convection. Finally, we propose scaling laws for the vertical convective heat flux, vertical velocity, and temperature perturbations.

KEYWORDS: Linear stability Mean-field approximation Radiative–convective model Radiative Rayleigh number Scaling laws Subcritical instability

1. INTRODUCTION

This paper uses an idealized model to advance understanding of atmospheres in radiative–convective equilibrium. Models that are idealized but that are derived from first principles have a special place in meteorology. For instance, the Eady model of baroclinic instability (Eady 1949), while artificial in some respects, has proved to be a valuable tool for understanding large-scale dynamics. Formulating equally simple models for radiative–convective atmospheres might also prove useful. Rayleigh–Bénard convection, in which a fluid layer is confined between upper and lower plates at fixed temperatures, does not suffice as a model of a radiative–convective atmosphere because it does not include radiation. Goody (1956) put forth a convective model that includes thermal radiation but also specifies the temperature on the boundaries. Although Goody's model is an instructive laboratory model, the atmosphere does not have an analogue to an upper lid at which temperature is fixed. Here we study a dry (cloud-free) model of atmospheric convection that includes radiative transfer, and specifies the radiative flux, rather than the temperature, at the top of the atmosphere. The goal is to move one step away from the Rayleigh–Bénard system and one step closer to atmospheric convection.

Since atmospheric convection is a response to instability (Emanuel 1994, p. 527), it is instructive to study the stability properties of radiative-equilibrium states. We find that the linear-stability properties of our model are similar to those of Rayleigh–Bénard convection. In particular, the threshold for marginal stability can be described in terms of a single parameter, a radiative Rayleigh number, which is similar to the classical Rayleigh number but incorporates effects of radiation.

The weakly nonlinear convecting properties of our radiative–convective system differ markedly from those of weakly nonlinear Rayleigh–Bénard convection. Specifically, the molecular viscosity and thermal diffusivity have little influence on the convective heat flux in the radiative–convective system, whereas they have a strong influence on weakly nonlinear Rayleigh–Bénard convection.

* Corresponding address: Cooperative Institute for Research in the Atmosphere, Colorado State University, Fort Collins, CO 80523-1375, USA. e-mail: larson@cira.colostate.edu

We propose buoyancy, velocity, and heat-flux scales for dry atmospheres in radiative–convective equilibrium. Recently, several authors have proposed bulk buoyancy and velocity scales for moist atmospheres (Craig 1996; Emanuel and Bister 1996; Rennó and Ingersoll 1996). These scales do not predict the vertical variation of buoyancy and velocity. For the simpler dry case, however, the vertical dependence of these quantities can be estimated.

2. LINEAR-STABILITY EQUATIONS

The set-up of our idealized radiative–convective model is summarized here. The atmosphere in our model consists of an infinite horizontal slab of fluid, bounded above and below by solid, free-slip boundaries at $z = 1$ and $z = 0$. Solar radiation illuminates the top of the atmosphere, passes through the atmosphere unimpeded, and is absorbed entirely at the ground. Its only effect is to establish the proper ground temperature; solar radiation does not appear in the model equations. The model does not include clouds. The albedo of clouds is crudely taken into account by adjusting the solar constant appropriately. One of the effects of latent heating is crudely simulated by setting the model's 'adiabatic' lapse rate to the approximate climatological average (6.5 K km^{-1}), as has been done in many convective adjustment calculations, instead of using the dry adiabatic lapse rate. An advantage of using a 6.5 K km^{-1} adiabatic lapse rate is that it yields a reasonable tropopause height in the weakly nonlinear calculations below. For simplicity, the two-stream, grey approximation of Goody (1995) is used to represent radiative transfer, despite the fact that real atmospheric gases are non-grey. The profile of the radiative absorption coefficient, which depends on the profiles of radiatively active gases such as water vapour, is specified. Therefore, the model contains no water vapour feedback. We use the Boussinesq approximation (Spiegel and Veronis 1960), strictly valid only for a shallow atmosphere, despite the fact that the atmosphere we model is deep.

The governing equations may be non-dimensionalized as follows. (In this paper, subscript asterisks shall denote dimensional quantities.) We use a length scale h_*, where h_* is the height of the domain, an as yet unspecified temperature scale $\mathcal{T}_*$, a radiative time scale $t_{\mathcal{T}*} \equiv 3\rho_* h_* c_{p*}/(16\sigma_* \mathcal{T}_*^3)$, a radiative-flux scale $16\sigma_* \mathcal{T}_*^4/3$, and a pressure scale $\rho_* h_* g_* \alpha_{T*} \mathcal{T}_*$. Here ρ_* is the (constant) density, c_{p*} the heat capacity at constant pressure, σ_* the Stefan–Boltzmann constant, g_* the acceleration due to gravity, and α_{T*} the thermal expansion coefficient. With the above non-dimensionalization, the momentum, heat, continuity, and radiative-transfer equations become, respectively,

$$\chi \frac{\partial \mathbf{v}}{\partial t} + \chi \mathbf{v} \cdot \nabla \mathbf{v} = -\gamma \nabla p' + \gamma T' \mathbf{k} + \nabla^2 \mathbf{v}, \tag{1}$$

$$\frac{\partial T}{\partial t} + \mathbf{v} \cdot \nabla T + w\Gamma = -\nabla \cdot \mathbf{F} + \kappa \nabla^2 T, \tag{2}$$

$$\nabla \cdot \mathbf{v} = 0, \tag{3}$$

and

$$\nabla \frac{1}{\alpha} \nabla \cdot \mathbf{F} - 3\alpha \mathbf{F} = \frac{3}{4} \nabla T^4. \tag{4}$$

Here $\mathbf{v}$ denotes the velocity vector, w the vertical component of velocity, T' the temperature perturbation from the basic state temperature, T the full temperature, $\mathbf{F}$ the (thermal) radiative flux, p' the perturbation pressure, t the time, α the specified non-dimensionalized radiative absorptivity field, and $\mathbf{k}$ the vertical unit vector. In addition,

the following non-dimensional parameters have been defined:

$$\gamma = \frac{g_* \alpha_{T*} \mathcal{T}_* h_*^3}{\nu_* (h_*^2 / t_{\mathcal{T}*})} \qquad \kappa = \frac{\kappa_*}{h_*^2 / t_{\mathcal{T}*}} \qquad \Gamma = \frac{\Gamma_* h_*}{\mathcal{T}_*} \qquad \chi = \frac{h_*^2 / \nu_*}{t_{\mathcal{T}*}}.$$

Here Γ_* is the adiabatic lapse rate, ν_* the kinematic viscosity, and κ_* the thermal diffusivity. We may interpret γ as a non-dimensional inverse viscosity, κ as a non-dimensional thermal diffusivity, and Γ as a non-dimensional adiabatic lapse rate. χ turns out not to enter the stability threshold.

The basic states whose stability properties we wish to investigate are motionless and horizontally uniform. Therefore $\mathbf{v} = 0$, $\overline{T} = \overline{T}(z)$, $\overline{\mathbf{F}} = \overline{F}_z(z)\mathbf{k}$, and $\alpha = \alpha(z)$. Substituting these forms into the heat equation (2) yields

$$0 = -\frac{\mathrm{d}\overline{F}_z}{\mathrm{d}z} + \kappa \frac{\mathrm{d}^2 \overline{T}}{\mathrm{d}z^2}. \tag{5}$$

When $\kappa = 0$, as in all stability calculations we perform, the basic state is a radiative equilibrium state in which heat is transported solely by radiation. Substituting $\overline{T}$, $\overline{\mathbf{F}}$, and α into the radiative-transfer equation (4) yields

$$\frac{\mathrm{d}}{\mathrm{d}z} \frac{1}{\alpha} \frac{\mathrm{d}\overline{F}_z}{\mathrm{d}z} - 3\alpha \overline{F}_z = 3\overline{T}^3 \frac{\mathrm{d}\overline{T}}{\mathrm{d}z}. \tag{6}$$

Linear-stability equations, for perturbations about the basic-state equations (5) and (6), can be formulated as follows. We apply the operator $\mathbf{k} \cdot \nabla \times \nabla \times$ to the momentum equation (1). This yields

$$\chi \frac{\partial}{\partial t} \nabla^2 w = \gamma \nabla_{\mathrm{h}}^2 T' + \nabla^2 \nabla^2 w + \{\mathbf{k} \cdot \nabla \times \nabla \times (\chi \mathbf{v} \cdot \nabla \mathbf{v})\}, \tag{7}$$

where $\nabla_{\mathrm{h}}^2 \equiv (\partial^2/\partial x^2 + \partial^2/\partial y^2)$ is the horizontal Laplacian. Next we subtract the basic state heat equation (5) from the full heat equation (2) and replace the divergence of the perturbation radiative flux with the Newtonian approximation,

$$\nabla \cdot \mathbf{F}' = rT' \qquad r = \frac{t_{\mathcal{T}*}}{t_{\mathrm{R}*}}, \tag{8}$$

where $t_{\mathrm{R}*} \equiv \rho_* h_* c_{p*} / (\sigma_* T_{\mathrm{e}*}^3)$ is the radiative time-scale of the atmosphere and $T_{\mathrm{e}*}$ is the emission temperature of the atmosphere. These manipulations yield

$$\frac{\partial T'}{\partial t} + w \left(\frac{\mathrm{d}\overline{T}}{\mathrm{d}z} + \Gamma \right) = -rT' + \kappa \nabla^2 T' + \{-\nabla \cdot (\mathbf{v} T')\}. \tag{9}$$

The first term on the right-hand side shows that radiation causes the 'radiative damping' of temperature perturbations, with a strength given by r.

For grey atmospheres, the Newtonian approximation is strictly valid only when the atmosphere is optically thin. However, we shall use the Newtonian approximation even for moderately thick atmospheres. We do so because, given its simplicity, the Newtonian approximation is remarkably accurate for the earth's (non-grey) clear-sky atmosphere, when temperature perturbations about the horizontal mean are small (Goody 1995, pp. 115–117). Our use of the Newtonian approximation should be viewed as a modelling assumption that enables us to better represent the earth's non-grey atmosphere with a grey radiative-transfer model.

To find the vertical velocity, W, and temperature, Θ', linear modes, we assume the following forms for the perturbations:

$$w = \mathrm{Re}\{W(z)f(x, y)e^{st}\} \qquad T' = \mathrm{Re}\{\Theta'(z)f(x, y)e^{st}\} \tag{10}$$

where $f(x, y)$, which describes the horizontal planform, satisfies

$$\nabla_h^2 f(x, y) = -a^2 f(x, y),$$

and a is a real, non-dimensionalized horizontal wave number. In general, $s = \sigma + i\omega$ can be complex. Substituting the modal forms, Eq. (10), into linearized versions of the equations for w, Eq. (7), and T', Eq. (9), yields, respectively,

$$\chi s(D^2 - a^2)W = -\gamma a^2\Theta' + (D^2 - a^2)^2 W \tag{11}$$

and

$$s\Theta' = -W\left(\frac{d\overline{T}}{dz} + \Gamma\right) - r\Theta' + \kappa(D^2 - a^2)\Theta', \tag{12}$$

where the operator $D \equiv d/dz$. Setting $\kappa = 0$ and eliminating Θ', we find an equation for W alone:

$$(s + r)\{s\chi - (D^2 - a^2)\}(D^2 - a^2)W = \gamma a^2\left(\frac{d\overline{T}}{dz} + \Gamma\right)W. \tag{13}$$

Larson (1999b) has shown, following the method of Spiegel (1962), that our radiative–convective system satisfies the principle of exchange of stabilities. Exchange of stabilities holds if the linear modes arise as steadily growing, overturning cells and not as an oscillatory instability. More precisely, exchange of stabilities is valid if, for any linear mode, the imaginary part of the growth rate, ω, is zero whenever the real part of the growth rate, σ, is zero (Drazin and Reid 1981, p. 12). Exchange of stabilities has also been proven for Rayleigh–Bénard convection (Pellew and Southwell 1940) and for various radiative–convective systems which specify the temperature on both boundaries, thereby departing from the radiative–convective system considered here (Spiegel 1960; Murgai and Khosla 1962; Davis 1969; Arpaci and Gőzűm 1973). However, it is not obvious, *a priori*, that exchange of stabilities also holds in our radiative–convective system. In the aforementioned systems, the basic-state lapse rate is everywhere unstably stratified. In an atmospheric radiative–convective system, however, the stratosphere is stably stratified. It thereby provides a restoring force for vertical motions and hence raises the possibility of oscillatory instability (Spiegel 1960). The fact that exchange of stabilities does hold demonstrates that this mechanism cannot lead to oscillatory instability in our model. The proof of Larson (1999b) is valid for both free-slip boundaries and no-slip boundaries, but is restricted to the case of zero thermal diffusivity.

3. An Analytic Linear-Stability Problem

The purpose of this section is to pose and analytically solve an idealized radiative–convective linear-stability problem which retains the simplicity of the Rayleigh–Bénard problem but is a somewhat more realistic model of the atmosphere. To construct a model of this simplicity requires several rather extreme modelling assumptions. The first is to linearize the thermal source function in the basic-state radiative-transfer equation about

the ground temperature T_{g*}, an approximation which introduces errors of roughly 40% into the radiative equilibrium state. Since, in this section, we choose the temperature scale $\mathcal{T}_* = T_{g*}$, linearizing the thermal source function amounts to setting the $\overline{T}^3$ factor in Eq. (6) equal to unity. Second, we set the radiative absorption coefficient, $\alpha = \alpha_c$, to be a constant with altitude, whereas the concentration of the atmosphere's main radiative absorber, water vapour, diminishes rapidly with altitude. Third, we place the solid, upper lid at the tropopause. Fourth, we set the thermal diffusivity, κ, to zero. In the atmosphere, the thermal diffusive damping is much smaller than radiative damping, and hence the $\kappa = 0$ results constitute an important limiting case. In the next section, we keep $\kappa = 0$ but relax the other assumptions. Some of the qualitative features of the present analytical model are preserved in the more sophisticated model.

First we write down the form of the basic state for the linear-stability analysis, leaving some constants undetermined. When $\kappa = 0$, the radiative–diffusive equilibrium, Eq. (5), reduces to a radiative equilibrium:

$$\overline{F}_z = F_T = \text{constant}$$

where F_T is the net outgoing thermal radiation at the top of the atmosphere, which equals the net incoming solar radiation. Inserting a constant radiative flux into the basic-state radiation equation (6), linearized about $\overline{T} = T_g = 1$, yields the basic-state temperature gradient

$$\frac{d\overline{T}}{dz} = -\alpha_c F_T = -(T_l - T_u). \tag{14}$$

A temperature discontinuity appears at the ground because thermal diffusivity is absent. T_l denotes the air temperature adjacent the ground, and T_u denotes the temperature at the top of the domain. The basic-state temperature decreases linearly with altitude.

Next we formulate radiative boundary conditions appropriate to the atmosphere. We stipulate that there is no incoming thermal radiation at the top of the domain. Then, following Goody (1995, pp. 114–115), we may show that the upper radiative boundary condition becomes

$$\tfrac{8}{3} F_T = \overline{T}^4\Big|_{z=1} \cong 1 - 4(1 - T_u). \tag{15}$$

The far right-hand side has been obtained by linearization about $\overline{T} = T_g = 1$. In a similar fashion, the bottom radiative boundary condition may be derived from the assumption that the upwelling radiance near the ground is that due to a black body. We find

$$\tfrac{8}{3} F_T = 1 - \overline{T}^4\Big|_{z=0} \cong 4(1 - T_l). \tag{16}$$

We may now solve for the basic-state temperature gradient and radiative flux. Equations (14), (15), and (16) yield

$$\frac{d\overline{T}}{dz} = -\frac{(3/8)\alpha_c}{2 + (3/2)\alpha_c} \qquad F_T = \frac{3/8}{2 + (3/2)\alpha_c}. \tag{17}$$

With the basic state in hand, we proceed to solve for the linear-stability eigenmodes and eigenvalues. The eigenvalue problem consists of Eq. (13) with s set equal to zero because of exchange of stabilities, free-slip boundary conditions, and the basic-state temperature gradient, Eq. (17). By inspection, we see that the eigenfunctions are

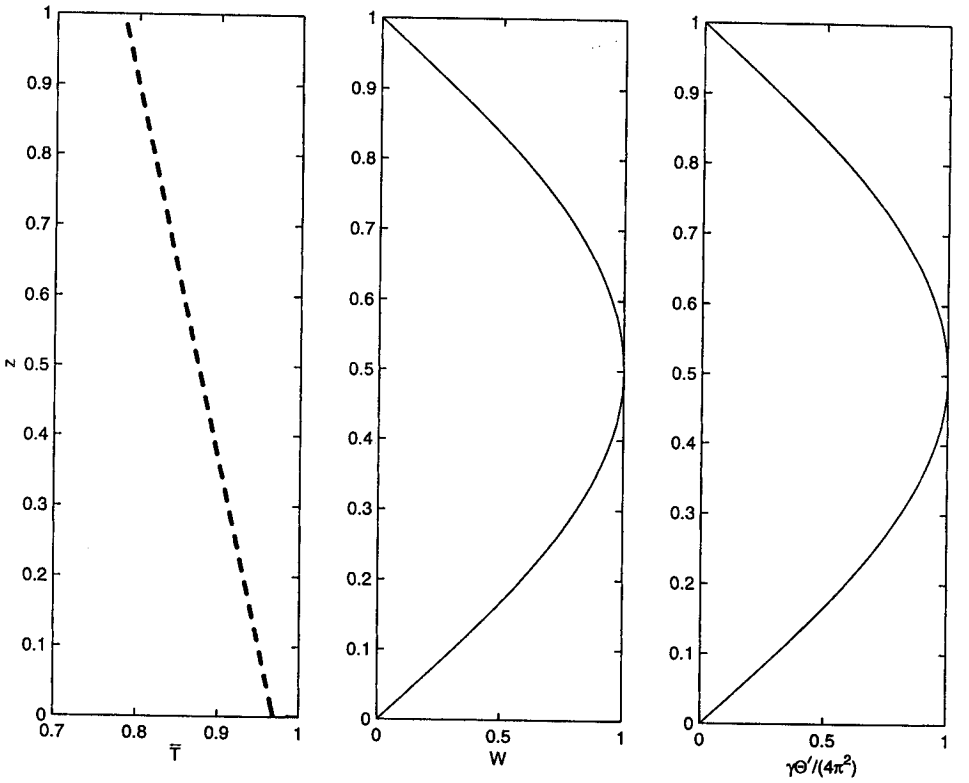

Figure 1. The basic state and eigenmodes plotted versus altitude for the analytic stability problem discussed in section 3. The left-hand panel displays the basic-state temperature profile $\overline{T}$, as computed from Eq. (17) (see text). There is a discontinuity at the ground. The middle panel displays the vertical-velocity eigenmode, and the right-hand panel displays the temperature-perturbation eigenmode. The eigenmodes are simple sinusoids, as in Rayleigh–Bénard convection, because $\overline{T}$ is linear in the interior. See text for further explanation.

sinusoidal and fill the depth of the layer, as in Rayleigh–Bénard convection. They are plotted, along with the basic-state temperature profile for $\alpha_c = 4$, in Fig. 1.

Our system has a critical wave number of $a = \pi$, similar to the critical wave number $a = \pi/\sqrt{2}$ for the Rayleigh–Bénard system. The critical threshold for marginal stability can be written in terms of a single parameter, a radiative Rayleigh number Ra_r. If we define a radiative diffusivity $\kappa_{R*} \equiv h_*^2/t_{R*}$, a lapse-rate difference from adiabatic

$$\beta_* \equiv -\frac{d\overline{T}_*}{dz_*} - \Gamma_* = \frac{3}{8}\frac{(F_{T*}/2\sigma_*)^{1/4}}{h_*}\left(\frac{\alpha_c^{4/3}}{2+(3/2)\alpha_c}\right)^{3/4} - \Gamma_*, \tag{18}$$

and a radiative Rayleigh number

$$Ra_r = -\left(\frac{d\overline{T}}{dz} + \Gamma\right)\frac{\gamma}{r} = \frac{g_*\alpha_{T*}\beta_* h_*^4}{\nu_*\kappa_{R*}}$$

$$= \frac{g_*\alpha_{T*}((3/8)\{(F_{T*}/2\sigma_*)^{1/4}/h_*\}[\alpha_c^{4/3}/\{2+(3/2)\alpha_c\}]^{3/4} - \Gamma_*)h_*^4}{\nu_*(h_*^2/t_{R*})}, \tag{19}$$

then the system is linearly unstable when Ra_r exceeds the critical value $Ra_{rC} = 4\pi^2$. Because of the simplifications we have introduced, the critical condition depends on

only one parameter, as in Rayleigh–Bénard convection. This parameter, Ra_r, resembles the classical Rayleigh number, except that κ_{R*} is a radiative diffusivity instead of the thermal diffusivity, and there is a temperature jump at the ground which is not included in β_*. The mathematics (and relatedly the mechanism) of this instability are similar to that for Rayleigh–Bénard convection, except that in our radiative–convective model, it is radiation, rather than thermal diffusivity, that causes thermal damping and largely determines the basic-state temperature profile. Spiegel (1960) and Larson (1999a) discuss similar radiative Rayleigh numbers for a system that resembles ours except that the temperatures of the boundaries are specified.

4. A LINEAR-STABILITY PROBLEM WITH AN EXPONENTIAL RADIATIVE ABSORPTION COEFFICIENT

We now perform a linear-stability analysis for a more realistic basic-state temperature profile. To produce a more realistic basic state, we relax some of the assumptions made in the analytical linear-stability problem (but retain the assumption of zero thermal diffusivity). First, the profile of the radiative absorption coefficient is no longer constant, but falls off exponentially with increasing altitude: $\alpha(z) = b \exp(-Sz)$, where S is a non-dimensional inverse scale height of absorption and b is a non-dimensional coefficient which sets the radiative absorptivity at the ground. This profile is intended to reflect the climatological profile of water vapour, the main radiative absorber. Second, the thermal source function in the radiative-transfer equation (6) is no longer linearized. Third, the upper lid is lifted to the lower stratosphere, so that the eigenmodes may freely penetrate the stable portion of the temperature profile. Also, in this section we choose the temperature scale to be $\mathcal{T}_* = \Gamma_* h_*$.

The basic state is a slight modification of that obtained by Goody (1995, pp. 126–127). The basic-state radiative flux is still constant, and a temperature discontinuity still appears at the ground. To obtain the temperature profile above the discontinuity, it is sufficient to solve Eq. (6) subject to the boundary condition, Eq. (15), where we no longer use the linearized approximation on the far right-hand side. We find

$$\overline{T} = \left(\frac{8}{3}F_T\right)^{1/4}\left(1 + \frac{3}{2}\frac{1}{S}(\alpha - be^{-S})\right)^{1/4}, \tag{20}$$

and, taking the derivative,

$$\frac{d\overline{T}}{dz} = -\frac{3}{8}\alpha\left(\frac{8}{3}F_T\right)^{1/4}\left(1 + \frac{3}{2}\frac{1}{S}(\alpha - be^{-S})\right)^{-3/4}. \tag{21}$$

The linear-stability problem consists of Eq. (13) with $s = 0$ and $d\overline{T}/dz$ given by Eq. (21), plus free-slip boundary conditions. We solve this eigenvalue equation with a pseudo-spectral Chebyshev numerical method, following Boyd (1989). Using linear combinations of Chebyshev polynomials, we construct a set of basis functions, each of which satisfies free-slip boundary conditions. We keep 102 basis functions. We expand W in terms of these basis functions and, given a choice of a^2, solve the eigenvalue problem for the coefficients. We compute all eigenvalues and select the smallest one. To find the critical value of γ, γ_C, we minimize the eigenvalue numerically with respect to a^2 using the golden section search (Press *et al.* 1992). Details of the numerical method are described in Larson (1999a).

We now compute the linear modes for a control run with $F_T = 2.75$, $b = 40$, and $S = 10$. If we assume the domain height is $h_* = 20$ km and the 'adiabatic' lapse rate

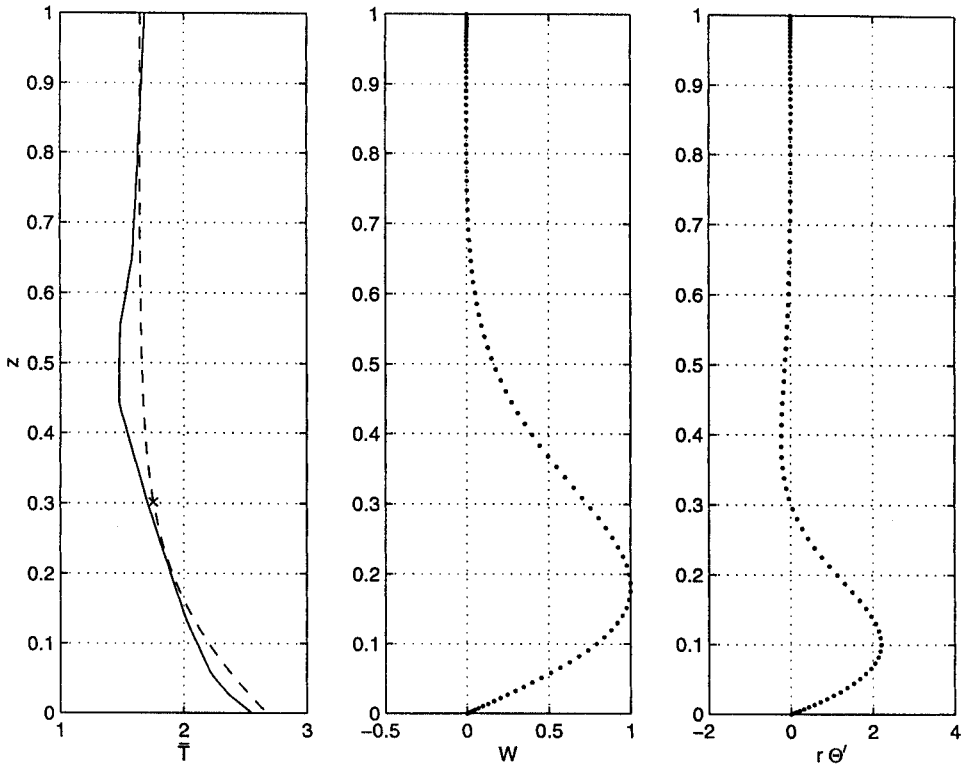

Figure 2. The basic state and critical linear eigenmodes of the radiative-equilibrium state discussed in section 4, for a control run with $F_T = 2.75$, $b = 40$, $S = 10$. The left-hand panel displays the basic-state temperature profile, Eq. (20), (dashed line) and, for comparison, the profile from Fig. 4 of Manabe and Strickler (1964) (solid line), divided by the temperature scale, $\Gamma_* h_* = 130$ K. Manabe and Strickler's calculation includes solar radiation, using annual-mean hemispheric values of the solar constant and zenith angle. The x-mark locates z_n, the top of the unstable portion of the dashed temperature profile. The middle panel shows the vertical-velocity eigenmode, and the right-hand panel shows the temperature-perturbation eigenmode multiplied by the radiative-damping parameter, r.

is $\Gamma_* = 6.5$ K km^{-1}, these values of the input parameters correspond roughly to the current globally averaged climate: net incoming solar radiation 240 W m^2, optical depth 4, and absorber scale height 2 km. Figure 2 depicts the basic-state temperature profile, $\overline{T}$, Eq. (20), along with the vertical velocity, W, and temperature, Θ', linear modes. Plotted along with $\overline{T}$ is a non-grey radiative-equilibrium profile from Manabe and Strickler (1964), calculated using climatological mid-latitude absorber profiles. The two basic states agree qualitatively except for the fact that Manabe and Strickler's temperature profile increases with height in the stratosphere. This is because they have included absorption of solar radiation by ozone, whereas we have not. The W mode exhibits a single, broad maximum, similar in shape to the sinusoidal W mode found in the analytic stability model. A notable feature of the W mode is that it penetrates far into the stably stratified portion of the basic state. The top of the unstably stratified portion of the basic state, $z_n = z_{n*}/h_*$, has been denoted by an x-mark in Fig. 2. z_{n*} is the altitude at which $-d\overline{T}_*/dz_* = \Gamma_*$. Whereas z_n corresponds to an altitude of about 6 km, W becomes small only at about 12 km and completely vanishes only at about 15 km. The W profile extends to (or above) the climatological tropopause, despite the fact that a linear mode is infinitesimal in amplitude and therefore has no inertia. Extensive overshooting of

linear modes into a stably stratified region was also found for non-radiative cases by Whitehead and Chen (1970) and Sun (1976). The Θ' mode is not sinusoidal, as in the analytical stability model, but instead has a large region of negative Θ' which arises because the mode penetrates into the stably stratified region.

We now seek the dependencies of the critical value, γ_C/r, on the governing parameters F_T, b, S. One could study how γ_C/r varies as the other parameters are varied individually, as depicted later in Fig. 4. The study of a three-dimensional parameter space, however, is unwieldy. Instead, prompted by the analytic stability problem, we characterize the stability properties in terms of a single parameter, another radiative Rayleigh number $Ra_{\mathcal{R}}$. Both Whitehead and Chen (1970) and Sun (1976) used modified Rayleigh numbers to characterize the stability of curved temperature profiles, but they did not include radiative damping or calculate their basic-state temperature profiles from radiative-equilibrium equations. To construct a useful Rayleigh number, we need to choose appropriate length, temperature-gradient, and heat-diffusivity scales. As a length scale, we choose z_{n*}, the depth of the unstably stratified portion of the basic state. (In contrast to Rayleigh–Bénard convection, h_* is not an appropriate length scale, since here convection does not penetrate to the top of the domain.) As a temperature-gradient scale β_*, we choose the average potential-temperature gradient across the unstably stratified portion of the basic state, excluding the discontinuity at the ground. Finally, as a diffusivity scale, we choose the radiative diffusivity z_{n*}^2/t_{R*}. Our radiative Rayleigh number is then defined as

$$Ra_{\mathcal{R}} \equiv \frac{g_* \alpha_{T*} \beta_* z_{n*}^4}{\nu_* (z_{n*}^2/t_{R*})} = \frac{\gamma}{r}\left(\frac{\Delta T}{z_n} - 1\right) z_n^2 \tag{22}$$

where

$$\beta_* = \frac{\Delta T_*}{z_{n*}} - \Gamma_*.$$

ΔT is the (non-dimensionalized) temperature drop across the unstably stratified portion of the basic state, excluding the temperature discontinuity at the ground. Note that $Ra_{\mathcal{R}}$ is independent of the height of the domain, h_*.

One cannot expect a single number to exactly encapsulate the stability properties of a curved basic-state temperature profile and, indeed, $Ra_{\mathcal{R}}$ serves only as an approximate measure of linear stability. $Ra_{\mathcal{R}}$ is inexact in large part because it contains no information about the temperature profile above z_{n*}. To determine the accuracy with which $Ra_{\mathcal{R}}$ indicates marginal stability, we start with the control-run values, $F_T = 2.75$, $b = 40$, and $S = 10$, vary each of these parameters one at a time over wide ranges, and then calculate $Ra_{\mathcal{R}C}$ and the critical wave number scaled by the depth of the unstable portion of the sounding $a_C z_n$. The results are summarized in Table 1. If $Ra_{\mathcal{R}}$ were a perfect measure of stability, the critical values of $Ra_{\mathcal{R}}$ in the fourth column would all be equal. In fact the values vary by roughly 12%. Hence it appears that $Ra_{\mathcal{R}}$ is an approximate, but still useful, measure of stability. The greatest deviations occur when S is varied, because varying S greatly alters the shape of the profile, and $Ra_{\mathcal{R}}$ contains little information about the shape. Values of the scaled critical wave number, $a_C z_n$, vary little. Therefore, the preferred wave length for linear instability remains approximately proportional to the depth of the unstable layer, z_n, as F_T, b, and S are varied.

The advantage of writing the stability threshold approximately in terms of the single parameter $Ra_{\mathcal{R}}$ is that one needs merely to inspect $Ra_{\mathcal{R}}$ in order to ascertain the approximate effects of the governing parameters on the stability threshold. For instance, inspection of $Ra_{\mathcal{R}}$ shows that increasing the radiative-damping time-scale, t_{R*},

TABLE 1. CRITICAL RADIATIVE RAYLEIGH NUMBERS AND WAVE NUMBERS

F_T	b	S	$Ra_{\mathcal{R}C}$	$a_C z_n$
2.75	40	10	30.50	2.24
0.6875	40	10	30.11	2.27
1.375	40	10	30.28	2.25
5.5	40	10	30.75	2.23
11.0	40	10	31.05	2.21
2.75	10	10	30.56	2.30
2.75	20	10	30.63	2.27
2.75	55	10	30.42	2.23
2.75	80	10	30.31	2.21
2.75	40	7	30.03	2.26
2.75	40	20	31.94	2.23
2.75	40	30	33.00	2.23
2.75	40	40	33.77	2.24

The radiative Rayleigh number, Eq. (22), evaluated at marginal stability, $Ra_{\mathcal{R}C}$, for various values of F_T (net outgoing thermal radiation at the top of the atmosphere), b (a non-dimensional coefficient which sets the radiative absorptivity at the ground), and S (inverse scale height of absorption). The critical wave number a_C times the depth of the unstable layer z_n is also listed. The first row contains the control-run values.

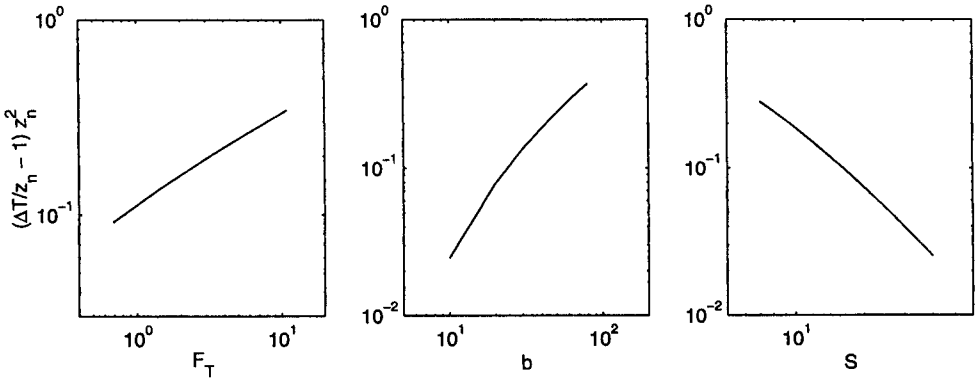

Figure 3. These panels illustrate the effect of F_T, b, and S on $(\Delta T/z_n - 1)z_n^2$ and hence their effect on the radiative Rayleigh number, $Ra_{\mathcal{R}} = (\gamma/r)(\Delta T/z_n - 1)z_n^2$. F_T, b, and S are each varied individually while the other two parameters are held fixed at the control-run values $F_T = 2.75$, $b = 40$, and $S = 10$. Increasing F_T or b destabilizes the basic state, whereas increasing S stabilizes the basic state. See text for further explanation.

destabilizes the radiative-equilibrium state, with an approximately linear dependence. The parameters which influence the basic state — F_T, b, and S — enter $Ra_{\mathcal{R}}$ only through the factor $(\Delta T/z_n - 1)z_n^2$. This factor's dependence on F_T, b, and S is plotted in Fig. 3. Increasing the net incoming solar radiation, F_T, destabilizes the radiative-equilibrium basic state. Similarly, increasing b, which corresponds to increasing the optical depth of the atmosphere while the shape of the absorber profile is held fixed, destabilizes the basic state. In both cases, it turns out that the destabilizations occur both because the depth of the unstable layer, z_n, increases and because the average lapse rate across z_n increases. Increasing S, which corresponds to decreasing the absorber

scale height, stabilizes the fluid by decreasing z_n. The present radiative Rayleigh number, $Ra_{\mathcal{R}}$, resembles the radiative Rayleigh number, Ra_r, for the constant absorption coefficient case. This, together with the similarity in W modes, indicates that the analytic solution for the constant absorption coefficient has qualitative relevance to the case when the absorption coefficient decreases with altitude.

$Ra_{\mathcal{R}}$, like Ra_r or the classical Rayleigh number Ra, may be interpreted as a measure of the relative strength of various dynamical terms (Tritton 1988, pp. 173–174). In particular, $Ra_{\mathcal{R}}$ may be regarded as the product of two ratios: the ratio of the buoyancy force over the viscous force, times the ratio of the advection of basic-state potential temperature over the radiative damping. The fact that instability in both the radiative–convective and Rayleigh–Bénard models can be described by types of Rayleigh numbers reflects the fundamental mechanistic similarity of linear instability in these models: what generates instability is hot fluid lying underneath cold fluid, and what suppresses instability is viscous and thermal damping. However, in the radiative–convective models, thermal damping is caused by radiative damping, not thermal diffusion, and the basic state is determined by radiation, not an imposed temperature difference across two plates and thermal diffusion. The value of our radiative–convective models is that they are almost as simple as the Rayleigh–Bénard model, but they illustrate how changes in radiative properties influence the stability of the system.

5. ENERGY-STABILITY THEORY

Linear-stability theory states that above a certain critical threshold — defined in the above models by either Ra_{rC} or $Ra_{\mathcal{R}C}$ — there exists a mode which grows, even if excited only infinitesimally. Linear-stability analysis does not establish, however, that beneath the critical threshold, the system is stable to large perturbations. Hence it does not establish whether or not subcritical instability can exist. In many atmospheric soundings, there are parcels of air that do not become positively buoyant until they are lifted to their level of free convection. Therefore, in some cases, moist convection arises as a subcritical instability (Emanuel 1994, pp. 168–169). However, even in a dry radiative–convective atmosphere, subcritical instability may still be possible if the basic-state temperature profile is curved.

The energy method is a nonlinear-stability method which provides information about whether or not subcritical instability can occur. The energy method determines a critical threshold below which any small or finite-amplitude perturbation, regardless of magnitude, decays. Beneath this threshold, the system is said to be monotonically stable. In the method, we define an 'energy' and derive an energy equation which contains generation and dissipation terms. Beneath the monotonic stability threshold, the dissipation terms are guaranteed to outweigh the generation terms, causing the energy to decay with time and rendering the system stable.

The threshold for monotonic stability either coincides with or lies below the critical threshold for linear stability. Beneath the monotonic-stability threshold, all disturbances decay; above the linear-stability threshold, at least one mode grows; but between the two thresholds, there is a region of indeterminate stability properties in which finite-amplitude subcritical instabilities may or may not exist. To reduce the region of indeterminacy, we seek to narrow the gap between the thresholds as much as possible.

For Rayleigh–Bénard convection, the basic-state temperature profile is linear, and Joseph (1965) was able to show that the thresholds coincide exactly, thereby proving that in this system no subcritical instabilities can occur. For the analytic problem of section 3, the basic-state temperature profile is also linear and one can prove in a similar

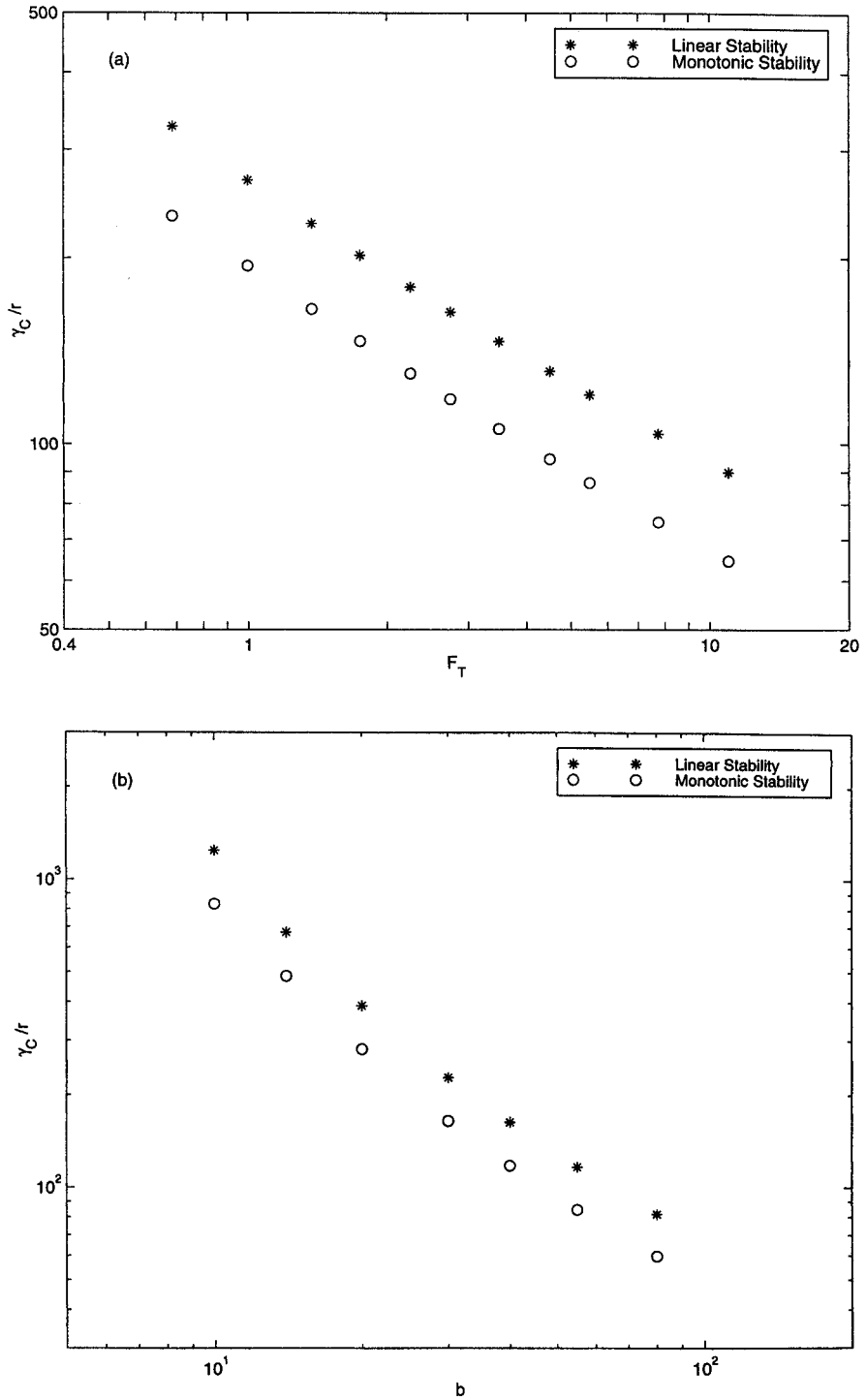

Figure 4. The critical threshold for linear stability, γ_C/r (asterisks), and the critical threshold for monotonic stability (circles) as computed from the energy method. One parameter at a time is varied, while the other parameters are held fixed at the control-run values, $F_T = 2.75$, $b = 40$, and $S = 10$. In (a), F_T is varied. In (b), b is varied. In (c), S is varied. See text for further explanation.

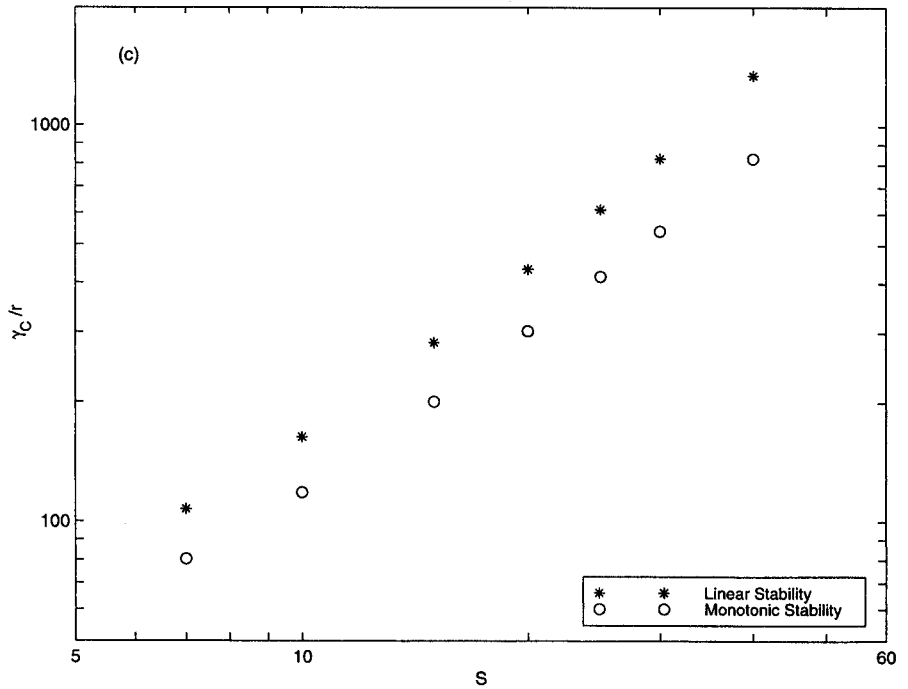

Figure 4. Continued.

manner that no subcritical instabilities exist (Larson 1999b). This is a strong result. The mathematics, which follow the methodology of Straughan (1992), are given in Larson (1999b) and will not be repeated here. Similar mathematics are also given in Larson (1999a) for a system which is like ours except that the temperatures on the boundaries are specified.

For the problem of section 4, the radiative-equilibrium temperature profile is nonlinear, and hence the result of the energy-method analysis differs from that for Rayleigh–Bénard convection. Namely, in the radiative problem, the monotonic-stability threshold lies somewhat below the linear-stability threshold (Larson 1999b). This is illustrated in Fig. 4, which shows plots of the monotonic-stability threshold (circles) superimposed on plots of the critical threshold, γ_C/r, for linear stability (asterisks). The linear-stability threshold is typically about 1.5 times greater than the monotonic-stability threshold. In the areas of parameter space between the monotonic- and linear-stability curves, there is the possibility of subcritical instability, although the analysis we have performed cannot confirm or deny this.

6. Development of the Mean-Field Equations

We now examine the behaviour of our radiative–convective system when weakly nonlinear convection occurs. To do so, we have chosen to use an approximation to the Boussinesq equations known as the mean-field approximation (Herring 1963, 1964; Musman 1968; Spiegel 1971). This approximation yields a set of equations which is one-dimensional and whose solutions, therefore, may be rapidly computed. Unlike many convective parametrizations, however, the mean-field equations are derived directly from the Boussinesq equations and do not rely on modelling assumptions like convective

adjustment. Furthermore, the mean-field equations provide individual profiles of the vertical velocity field, w, and the temperature-perturbation field, T', in addition to their correlation, the heat flux, $\overline{wT'}^{\mathrm{m}}$, where $\overline{(\,)}^{\mathrm{m}}$ denotes the horizontal mean. However, the mean-field equations are valid only for weakly nonlinear, high-Prandtl-number flows, whereas the atmosphere is strongly nonlinear and has a moderate Prandtl number.

We now outline a derivation of the mean-field equations. (For a more complete derivation, see Herring (1963), (1964).) Horizontal averages (means) can be taken over fields in the convecting state, and the mean fields are distinct from basic-state fields, which have been denoted by an overbar. An equation for the mean radiative flux $\overline{F_z}^{\mathrm{m}}$ may be derived as follows. We assume that the radiative absorption coefficient, $\alpha = b \exp(-Sz)$, decreases exponentially with height, where b and S are specified parameters. To a good approximation, the non-dimensionalized thermal source function in the radiative-flux equation (4) may be linearized about the local horizontal mean:

$$T^4 \cong \overline{T}^{\mathrm{m}4} + 4\overline{T}^{\mathrm{m}3}T'.$$

Then, since α is a function of z alone, horizontally averaging the radiative-flux equation (4) yields Eq. (6), except that basic-state quantities are replaced by mean quantities. To find an equation for $\overline{T}^{\mathrm{m}}$, we substitute $T = \overline{T}^{\mathrm{m}}(z) + T'$ into the heat equation (2) and average over the horizontal:

$$\frac{\partial \overline{T}^{\mathrm{m}}}{\partial t} = -\frac{\mathrm{d}\overline{F_z}^{\mathrm{m}}}{\mathrm{d}z} + \kappa \frac{\mathrm{d}^2\overline{T}^{\mathrm{m}}}{\mathrm{d}z^2} - \frac{\mathrm{d}\overline{wT'}^{\mathrm{m}}}{\mathrm{d}z}. \tag{23}$$

We have assumed that $\overline{w}^{\mathrm{m}} = 0$. To form an equation for the temperature perturbation from the mean, we subtract the mean-temperature equation (23) from the heat equation (2) and use the Newtonian approximation, Eq. (8). This yields Eq. (9), except that basic-state quantities are replaced by mean quantities, and the bracketed term becomes $\{-\nabla \cdot (\mathbf{v}T') + \mathrm{d}(\overline{wT'}^{\mathrm{m}})/\mathrm{d}z\}$. For the mean-field calculations, we shall choose the temperature scale $\mathcal{T}_* = \Gamma_* h_*$. Then the non-dimensionalized adiabatic lapse rate Γ is unity. Our equation for w is (7).

Now we neglect the fluctuating self-interaction terms (i.e. the bracketed terms) in the equations for w and T'. The neglect of these terms restricts the scope of the system to weakly nonlinear, high-Prandtl-number flows. With the neglect of the self-interaction terms, the mean-field equations for w and T' become identical to linear-stability equations for the *mean* temperature field $\overline{T}^{m}$ (Howard 1964). However, the mean-field equations do retain some nonlinearity: namely, they retain the $\mathrm{d}(\overline{wT'}^{\mathrm{m}})/\mathrm{d}z$ term in the mean heat-flux equation (23) and the $w\mathrm{d}\overline{T}^{\mathrm{m}}/\mathrm{d}z$ term in the temperature-perturbation equation (9). Convective heating is permitted to alter $\overline{T}^{\mathrm{m}}$, whose modified profile can then affect the other fields.

Only one horizontal mode is retained, whose horizontal planform is described by the function $f(x, y)$ as in the linear-stability analysis (Eq. (10), with $s = 0$; this assumes perfect horizontal correlation between w and T'). Now, however, we also impose the normalization condition $\overline{f^2}^{\mathrm{m}} = 1$. In the mean-field equations, the horizontal wave number, a, is a free parameter. We choose the value of a used in a mean-field calculation to be the critical wave number obtained from a linear-stability calculation for the same system with the same or similar values of the governing parameters. We focus exclusively on steady-state solutions. Assuming a steady state and substituting the modal forms, Eq. (10), with $s = 0$ into the equations for w and T' yields, respectively, Eq. (11) and Eq. (12), but with $s = 0$, $\Gamma = 1$, and $\overline{T}$ replaced by $\overline{T}^{\mathrm{m}}$.

We impose the following boundary conditions. The upper and lower boundaries are located at $z = 0$ and $z = 1$ and are taken to be free-slip. Since we permit non-zero thermal diffusivity, we must impose boundary conditions on temperature. At the top of the domain, we set $\mathrm{d}T/\mathrm{d}z|_{z=1} = 0$ so that the temperature at the top boundary can vary freely. At the bottom boundary, we specify the temperature, $T|_{z=0} = T_g$, and then compute the outgoing radiative flux at the top of the domain, F_T. Conceptually, however, it is simpler to regard F_T as an external parameter and T_g as an internally determined one. Therefore, in the experiments described herein we shall specify F_T and then perform a numerical search to find the ground temperature, T_g, which yields the desired radiative flux at the top. We derive the boundary conditions on radiative flux following the procedure of Goody (1956, 1995). We find

$$\left.\frac{1}{\alpha}\frac{\mathrm{d}\overline{F}_z^{\mathrm{m}}}{\mathrm{d}z} - 2\overline{F}_z^{\mathrm{m}}\right|_{z=0} = 0, \tag{24}$$

which assumes a black lower surface, and

$$\left.\frac{1}{\alpha}\frac{\mathrm{d}\overline{F}_z^{\mathrm{m}}}{\mathrm{d}z} + 2\overline{F}_z^{\mathrm{m}}\right|_{z=1} = \left.\frac{3}{4}\overline{T}^{\mathrm{m}4}\right|_{z=1}, \tag{25}$$

which states that there is no incoming thermal radiation into the top of the domain.

The mean-field equations are solved numerically, following Boyd (1989). To resolve the thin boundary layers which form in $\overline{T}^{\mathrm{m}}$ and Θ', we expand all fields in Chebyshev polynomials, modified to span the interval $z = (0, 1)$. For most runs, we retain 100 polynomials, but when necessary we use 200 polynomials. The boundary conditions are imposed with the 'boundary-bordering' method described by Boyd (1989). To compute the solutions, we choose a first-guess solution, linearize the equations about this solution, and then solve for the perturbations iteratively, using Newton's method (Press *et al.* 1992). Newton's method converges only if a sufficiently close first-guess solution is postulated. When γ is just supercritical, we use the radiative-equilibrium solution as a first guess for $\overline{T}^{\mathrm{m}}$ and $\overline{F}_z^{\mathrm{m}}$, and the linear modes as a first guess for W and Θ'. To find highly supercritical solutions, we use the continuation method. That is, we use the mean-field solution for a low value of γ as a first-guess solution for a slightly higher value of γ. We continue to march in this way to higher and higher values of γ.

We illustrate the solutions of the mean-field equations with the output of a control run based on the following parameter values: $F_T = 2.75$, $r = 17$, $b = 40$, $S = 10$, $a^2 = 45.2$, $\gamma = 7 \times 10^5$, and $\kappa = 1/30$. If we take the height of the domain to be $h_* = 20$ km and the 'adiabatic' lapse rate to be $\Gamma_* = 6.5$ K km^{-1}, then these parameter values correspond approximately to the following dimensional quantities, assuming reasonable values for the air density, heat capacity, and so forth: net incoming solar radiation 238 W m^{-2}, Newtonian cooling time-scale of 10 days, optical depth of 4, and scale height of radiative absorber (i.e. water vapour) 2 km. Because the mean-field equations are valid only for weakly nonlinear flows and because very fine resolution is required for highly nonlinear flows, we cannot reach the values of γ and κ appropriate to the atmosphere, if molecular values of ν_* and κ_* are assumed.

$\overline{T}^{\mathrm{m}}$, W, Θ', and components of the heat flux are plotted in Fig. 5. The $\overline{T}^{\mathrm{m}}$ profile corresponds to a tropopause height of about 11.5 km and a nearly isothermal lower stratosphere with temperature 209 K. The tropospheric lapse rate is nearly the adiabatic lapse rate. The nearly neutral troposphere has not been specified *a priori*, as in convective adjustment calculations, but emerges from the calculation instead. This indicates

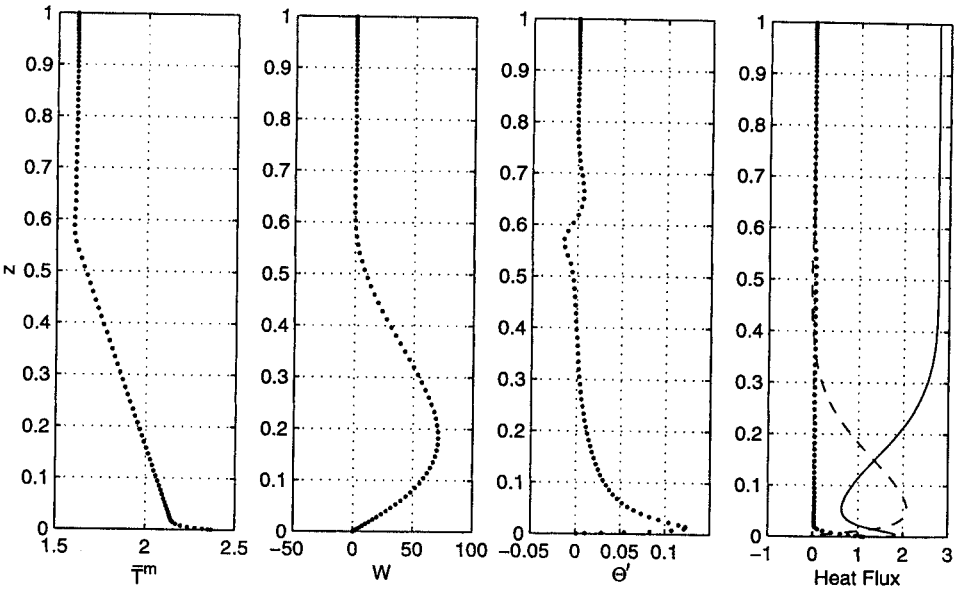

Figure 5. The mean temperature, $\overline{T}^m$, vertical velocity, W, temperature perturbation Θ', and components of the heat flux obtained from the mean-field equations. In the far right-hand panel, the radiative flux, $\overline{F}_z^m$, is denoted by a solid line, convective heat flux, $\overline{wT'}^m$, by a dashed line, and diffusive heat flux, $-\kappa d\overline{T}^m/dz$, by a dotted line. The vertical velocity and temperature-perturbation fields are periodic in the horizontal; the ascending branch is displayed here. This is a control run with parameter values $F_T = 2.75$, $b = 40$, $S = 10$, $r = 17$, $\kappa = 1/30$, $\gamma = 7 \times 10^5$, and $a^2 = 45.2$. The mean lapse rate is nearly adiabatic in the troposphere, and W has a single, broad maximum, as in the linear-stability calculations. See text for further explanation.

that although the convection is weakly nonlinear, it is strong enough to lead to a nearly neutral tropospheric lapse rate. Although the aforementioned features are in reasonable agreement with the current average climate, there is a very large and unrealistic (~29 K) jump in $\overline{T}^m$ at the lower boundary. This jump, we believe, results primarily from the absence of evaporation in this dry model (although turbulent mixing may also reduce the size of the jump). Large temperature jumps do exist in the earth's climate over dry regions such as the Sahara desert, due to a lack of evaporative cooling at the surface (Pierrehumbert 1995). The temperature (279 K) just above the jump and the earth's average surface temperature (about 288 K) are fairly close.

Comparing Figs. 2 and 5, we see that the linear-stability W mode has turned out to resemble the mean-field W profile in several respects. The linear W mode penetrates roughly as high as (but actually slightly higher than) the mean-field W profile. Therefore, convection does not penetrate further upwards as viscosity decreases, at least not while the convection is still weakly nonlinear. Both the linear W mode and the mean-field W exhibit a single, broad maximum in the mid troposphere. Both W profiles also qualitatively resemble the atmospheric boundary-layer data of Stull (1988, Figure 4.2) compiled from observations and numerical computations. In these data, the variance of vertical velocity has a single, broad maximum.

The shape of the mean-field Θ' profile can be rationalized once $\overline{T}^m$ and W are known. For example, the positive spike in Θ' near the ground is a consequence of upward motion in the presence of the super-adiabatic region near the ground. There are also some small wiggles in Θ' near the tropopause. The negative bump in Θ' is due to rising motion in the stably stratified region near the tropopause. A very weak reverse

cell in W, almost invisible on the plot, begins just above the tropopause. The positive bump in Θ' above the tropopause arises from subsidence warming in this reverse cell.

The far right-hand panel of Fig. 5 depicts the mean-field conductive, convective, and radiative vertical heat fluxes. In a steady state, these three fluxes must sum to a constant with altitude (see Eq. (23)). The sharp increase in $\overline{wT'}^{m}$ near the ground is balanced by sharp decreases in the conductive and radiative fluxes. Above this boundary layer, $\overline{F_z}^{m}$ increases roughly linearly, $\overline{wT'}^{m}$ decreases roughly linearly, and the diffusive heat flux is negligible. $\overline{wT'}^{m}$ is mostly positive, but does contain a vertically extensive region near the tropopause of weak negative heat flux.

Following Musman (1968), we have performed an *a posteriori* check of the validity of neglecting the self-fluctuating interaction terms in the equations for T' and w. The nonlinear term in the equation for w may be made as small as desired by choosing a sufficiently large Prandtl number. Hence the mean-field approximation restricts us to the high-Prandtl-number limit. The neglected terms in the equation for T' appear to affect the solution quantitatively, but not qualitatively, for typical parameter values in this study.

7. Dependence of the Convective Heat Flux on the Governing Parameters

The six external parameters in our radiative–convective problem may be placed into two groups. One group consists of the three 'basic-state parameters' — b, S, and F_T — that help determine the radiative-equilibrium state. The other group consists of three 'damping parameters' — γ, κ, and r — that do not affect the radiative-equilibrium basic state. The numerical calculations show that the basic-state parameters have a strong effect on $\langle wT' \rangle$, but the damping parameters have only a weak influence on $\langle wT' \rangle$. (Angled brackets, $\langle\ \rangle$, denote a spatial average over the entire fluid domain.) In the latter respect, the radiative–convective system differs markedly from weakly nonlinear Rayleigh–Bénard convection. An explanation for the weak effect of the damping parameters is offered in this section.

An example of the strong effect of the basic-state parameters on $\langle wT' \rangle$ is shown in Fig. 6. In this figure, all parameters except F_T are fixed at the control run values. To a crude approximation, $\langle wT' \rangle \sim F_T$, as might have been anticipated on dimensional grounds. The other basic-state parameters also strongly influence $\langle wT' \rangle$. Specifically, $\langle wT' \rangle$ increases with increasing b (for typical values of b) and increases with decreasing S (not shown). The increases in $\langle wT' \rangle$ occur because either an increase in b or a decrease in S leads to an increase in optical depth and tropopause height.

However, the damping parameters have little effect on $\langle wT' \rangle$, for sufficiently weak damping. This is illustrated for the thermal diffusivity κ in Fig. 7. Here all parameters are fixed at the control-run values except κ. If the three points in Fig. 7 with the highest values of $\langle wT' \rangle$ are fitted to a power law, the exponent is about -0.018. This may be compared with the order-unity exponent for F_T. Similarly, γ (which goes as $1/\nu_*$) and the radiative damping parameter, r, have little effect on $\langle wT' \rangle$ (not shown). (It is only the radiative damping of temperature perturbations which has little importance; the radiative cooling due to the mean-temperature profile strongly constrains $\langle wT' \rangle$.) However, the values of the damping parameters, even when small, do influence the individual profiles of w and T'. For instance, when viscosity is small, decreasing viscosity, while holding all other parameters fixed, increases w and decreases T' but keeps $\langle wT' \rangle$ approximately constant.

In contrast, the values of the molecular viscosity, ν_*, and thermal diffusivity, κ_*, have a strong influence on the heat flux in weakly to moderately nonlinear Rayleigh–Bénard

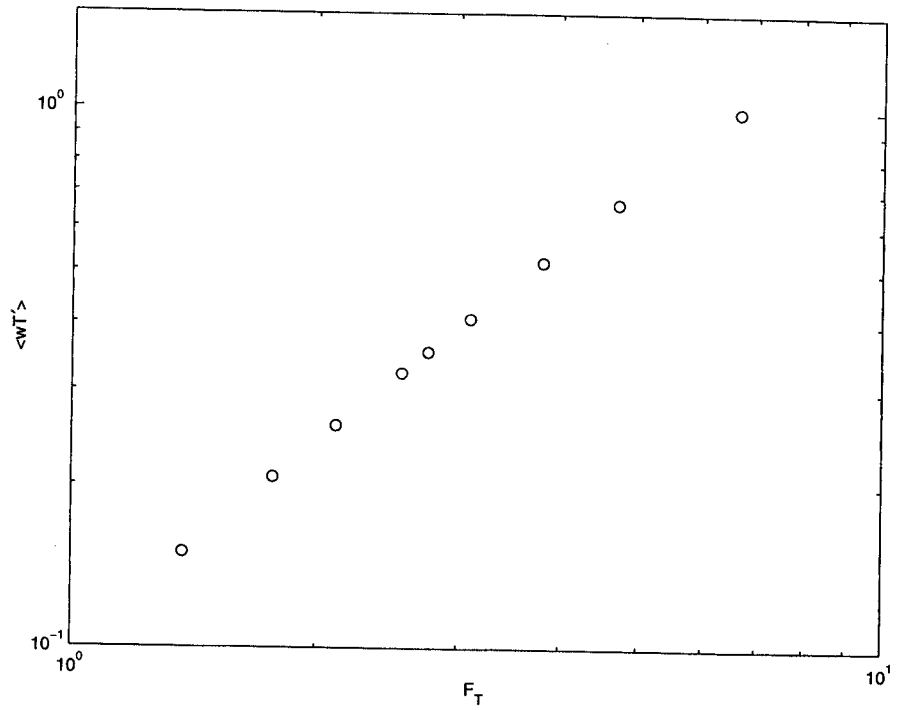

Figure 6. The domain-averaged convective heat flux, $\langle wT' \rangle$, versus the net incoming solar radiation, F_T. The other governing parameters are fixed at the control-run values.

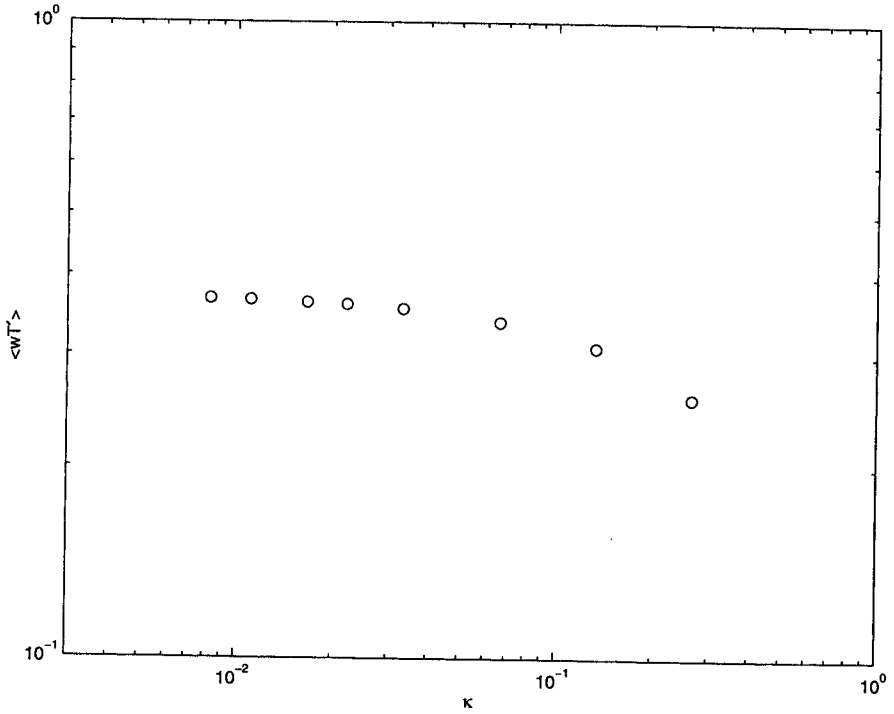

Figure 7. The domain-averaged convective heat flux, $\langle wT' \rangle$, versus the thermal diffusivity, κ. The other governing parameters are fixed at the control-run values.

convection. Several early experiments and theories (Malkus 1954; Chan 1971; Herring 1963; Spiegel 1971), including mean-field theory, suggested that the heat flux scales as $Ra^{1/3}$. Other experiments found a $Ra^{2/7}$ scaling (Castaing *et al.* (1989); see also Siggia (1994)). Both exponents imply that the dimensional heat flux depends on the values of ν_* and κ_*. (However, Kraichnan (1962) has theorized that at very high Rayleigh numbers (roughly $\geqslant 10^{24}$), a $Ra^{1/2}$ scaling with logarithmic corrections should result; this is the exponent which implies no dependence on a change in ν_* and κ_*, if the Prandtl number is held fixed.)

The issue of whether or not atmospheric flows depend on the values of the damping parameters is an important one. If the damping parameters were to matter, then meteorological theory would be complicated by, for instance, the introduction of extra parameters into dimensional analyses. Furthermore, molecular effects on atmospheric turbulence cannot be studied by explicit numerical computation, since atmospheric models cannot resolve the smallest fluid scales. Prior work has suggested various reasons why atmospheric convection might not depend on molecular quantities. For instance, the ground is invariably rough, and an externally induced mean wind usually blows over the surface (Emanuel 1994, pp. 88–91). Also, atmospheric convection itself may generate significant mechanical turbulence near the ground, as suggested by the mixing-length argument of Kraichnan (1962). All these factors might sufficiently disrupt the micro-layer near the earth's surface to destroy the bottleneck in heat flux near the surface that gives rise to the dependence on molecular quantities. The system we study has neither a rough lower surface nor a mean wind nor a high degree of turbulence, and yet the convective heat flux still depends only weakly on viscosity and thermal diffusivity. Therefore, our model results suggest that there exists an independent mechanism which renders viscosity and thermal diffusivity unimportant for atmospheres in radiative–convective equilibrium. An advantage of this latter mechanism is that, unlike the others, it can be easily investigated via simple numerical calculations.

The mechanism may be understood as follows. First, we note that in the interior of the troposphere, convective heating is almost entirely balanced by radiative cooling. Mathematically, this may be expressed by assuming a steady state, integrating the mean heat-flux equation (23) vertically, and neglecting thermal diffusivity:

$$\overline{wT'}^{\mathrm{m}} = F_{\mathrm{T}} - \overline{F}_z^{\mathrm{m}}. \tag{26}$$

Therefore, if the net incoming solar radiation, F_{T}, and the radiative flux, $\overline{F}_z^{\mathrm{m}}$, are independent of the damping parameters, so is the convective heat flux. In our model, F_{T} is fixed. (In the real atmosphere, F_{T} would depend on the damping parameters if, for example, the cloud albedo were to do so.) Furthermore, $\overline{F}_z^{\mathrm{m}}$ is determined entirely by the radiative absorption coefficient, α, and $\overline{T}^{\mathrm{m}}$ (see Eqs. (6), (24) and (25)). Therefore, the convective heat flux is independent of the damping parameters if α and $\overline{T}^{\mathrm{m}}$ are. But α is fixed in our model. (In the real atmosphere, α would depend on the damping parameters if the water-vapour profile were to do so.) $\overline{T}^{\mathrm{m}}$ is strongly constrained to follow an adiabatic lapse rate in the troposphere and a radiative-equilibrium profile in the stratosphere. Thus, for sufficiently weak damping, a change in the damping parameters is unlikely to alter $\overline{T}^{\mathrm{m}}$ appreciably. We conclude that the damping parameters have only a weak influence on $\langle wT' \rangle$, for sufficiently weak damping. It is worth noting that the mechanism depends in part on the fact that it is the flux, F_{T}, that is specified at the top of the atmosphere, not the temperature. The residual weak dependence is caused partly by the fact that κ and γ do affect $\overline{T}^{\mathrm{m}}$ near the ground, specifically in

the magnitude of the sharp jump there. The effect is weak because the atmosphere is optically thick and hence the mean temperature near the surface is only loosely coupled to temperatures aloft. (Since real atmospheric gases are non-grey, the ground temperature can be communicated to higher altitudes through relatively transparent regions in the spectrum. However, over most of the earth's surface, there is strong evaporation, which tends to eliminate any temperature jump at the surface. Hence for the real atmosphere we would again expect κ and γ to have little importance.) Spiegel (1971) has invoked similar reasoning to suggest that convection in stars does not depend on viscosity or thermal diffusivity.

In our model, as the damping decreases, the convective heat flux slowly increases. However, even when the damping becomes infinitesimally small, one can still place an upper bound on the magnitude of the convective heat flux. Specifically, Larson (1999b) has proved that for our idealized, steady-state system, $\overline{wT'}^{\mathrm{m}} < F_{\mathrm{T}}$ everywhere, if $\mathrm{d}\overline{T}^{\mathrm{m}}/\mathrm{d}z < 0$ everywhere. The proof is by construction: using the Green's function for the radiative-transfer equation (6), one finds an expression for $\overline{F}_z^{\mathrm{m}}$ in terms of the temperature profile; inspection of this expression reveals that $\overline{F}_z^{\mathrm{m}} > 0$. Then the conclusion follows easily from the mean vertical heat-flux equation. Larson (1999b) also extends the proof to write (loose, but rigorous) upper and lower bounds on $\langle wT' \rangle$. Namely, in our steady-state radiative–convective model, the integrated convective heat flux must fall within the range $0 \leqslant \langle wT' \rangle < F_{\mathrm{T}}$, if $\mathrm{d}\overline{T}^{\mathrm{m}}/\mathrm{d}z < 0$ everywhere. Because of the constraints imposed by radiation, deriving an upper bound on heat flux turns out to be straightforward, given that the temperature everywhere decreases with altitude. Establishing an upper bound on heat flux in Rayleigh–Bénard convection requires much more effort (Malkus 1954; Howard 1963).

8. Scaling laws

We now derive two scalings for $\langle wT' \rangle$, a sophisticated one and a simpler one. We begin by noting that Fig. 5 shows that in the middle troposphere, thermal diffusion is negligible, and $\overline{wT'}^{\mathrm{m}}$ decreases roughly linearly with altitude. Then dimensional reasoning and mixing-length theory applied to the mean heat-flux equation (23) both suggest the following expression for the convective heat flux:

$$\begin{aligned} \overline{wT'}^{\mathrm{m}} &\sim \frac{\mathrm{d}\overline{F}_z^{\mathrm{m}}}{\mathrm{d}z}(z_{\mathrm{n}} - z) \qquad && 0 < z < z_{\mathrm{n}} \\ &\cong 0 && z \geqslant z_{\mathrm{n}}. \end{aligned} \tag{27}$$

The depth of the radiative-equilibrium unstable layer, z_{n}, may be regarded as an external parameter, since an approximation to z_{n} for small κ can be expressed in terms of the external parameters b, S, and F_{T} via Eq. (21). (Although in our model b and S are external parameters, in the earth's atmosphere they are not.)

We still need to express $\mathrm{d}\overline{F}_z^{\mathrm{m}}/\mathrm{d}z$ in terms of external parameters. To do so, we rearrange the radiative-transfer equation (6) as follows

$$\overline{F}_z^{\mathrm{m}} = \frac{1}{\alpha}\left(-\overline{T}^{\mathrm{m}3}\frac{\mathrm{d}\overline{T}^{\mathrm{m}}}{\mathrm{d}z}\right) + \frac{1}{3}\frac{1}{\alpha}\frac{\mathrm{d}}{\mathrm{d}z}\frac{1}{\alpha}\frac{\mathrm{d}\overline{F}_z^{\mathrm{m}}}{\mathrm{d}z} \tag{28}$$

and apply $\mathrm{d}/\mathrm{d}z$ to both sides. The derivative of the first term on the right-hand side can be crudely approximated as

$$\frac{\mathrm{d}}{\mathrm{d}z}\frac{1}{\alpha}\left(-\overline{T}^{\mathrm{m}3}\frac{\mathrm{d}\overline{T}^{\mathrm{m}}}{\mathrm{d}z}\right) \cong S\frac{1}{\alpha}\left(-\overline{T}^{\mathrm{m}3}\frac{\mathrm{d}\overline{T}^{\mathrm{m}}}{\mathrm{d}z}\right) \cong S\overline{F}_z^{\mathrm{m}} \sim SF_{\mathrm{T}}. \tag{29}$$

The first equality holds because the radiative absorption coefficient, $\alpha = b\exp(-Sz)$, varies more rapidly with altitude than $\overline{T}^{\mathrm{m}3}\mathrm{d}\overline{T}^{\mathrm{m}}/\mathrm{d}z$. The second equality holds because it turns out that, in our numerical calculations for low to moderate S, the second term on the right-hand side of Eq. (28) is the smallest.

The derivative of the second term on the right-hand side of Eq. (28) can be crudely scaled using the standard mixing-length procedure of replacing derivatives by length scales. We find

$$\frac{1}{3}\frac{\mathrm{d}}{\mathrm{d}z}\left(\frac{1}{\alpha}\frac{\mathrm{d}}{\mathrm{d}z}\frac{1}{\alpha}\frac{\mathrm{d}\overline{F}_z^{\mathrm{m}}}{\mathrm{d}z}\right) \cong -\frac{1}{3}\frac{S}{z_{\mathrm{n}}}\frac{1}{\alpha^2}\frac{\mathrm{d}\overline{F}_z^{\mathrm{m}}}{\mathrm{d}z}. \tag{30}$$

In this problem, mixing-length theory has two length scales at its disposal: $1/S$ and z_{n}. We have used both length scales because doing so yields a better fit. The minus sign arises because of the curvature in $\overline{F}_z^{\mathrm{m}}$. We need to choose an altitude at which to evaluate α. This altitude is effectively a fitting coefficient, which we choose to be $z = z_{\mathrm{n}}/2$.

Combining Eqs. (28), (29), and (30), and solving for $\mathrm{d}\overline{F}_z^{\mathrm{m}}/\mathrm{d}z$, we find

$$\frac{\mathrm{d}\overline{F}_z^{\mathrm{m}}}{\mathrm{d}z} \sim \frac{F_{\mathrm{T}}S}{1 + (1/3)(S/z_{\mathrm{n}})(1/b^2)\mathrm{e}^{Sz_{\mathrm{n}}}}. \tag{31}$$

This scale for the radiative cooling, $\mathrm{d}\overline{F}_z^{\mathrm{m}}/\mathrm{d}z$, may be interpreted as a radiative scale, F_{T}, divided by a length scale, $1/S$, modified by the correction factor in the denominator. Substituting this radiative-cooling scale into Eq. (27) yields the scaling:

$$\begin{aligned}\overline{wT'}^{\mathrm{m}} &= c_1\frac{F_{\mathrm{T}}S}{1 + (1/3)(S/z_{\mathrm{n}})(1/b^2)\mathrm{e}^{Sz_{\mathrm{n}}}}(z_{\mathrm{n}} - z) \qquad 0 < z < z_{\mathrm{n}} \\ &= 0 \qquad\qquad\qquad\qquad\qquad\qquad\qquad\qquad z \geqslant z_{\mathrm{n}},\end{aligned} \tag{32}$$

where c_1 is a constant. Integrating over the domain,

$$\langle wT'\rangle = 0.5c_1\frac{F_{\mathrm{T}}S}{1 + (1/3)(S/z_{\mathrm{n}})(1/b^2)\mathrm{e}^{Sz_{\mathrm{n}}}}z_{\mathrm{n}}^2. \tag{33}$$

The most important features of this scale are that it has an explicit linear dependence on F_{T} and no explicit dependence on the damping parameters. A simpler scaling may be derived by neglecting the second term on the right-hand side of Eq. (28). This results in the same scalings as Eqs. (31), (32), and (33), except that the denominator in these scales is set to unity. Hence the simpler radiative-cooling scale can be directly interpreted as a radiative-flux scale divided by a length scale.

In Fig. 8, we test the scaling, Eq. (33), and its simpler variant against mean-field solutions. In this figure, we vary a single parameter while fixing all others at their control-run values. We do this for variables F_{T}, b, γ, κ, and r. When we vary S, however, we also vary a^2. As S is varied, the depth z_{n} of the unstable portion of the basic state varies markedly, and hence the wavelength of the most unstable linear mode also varies greatly. For each value of S in Fig. 8, we choose a to be the critical wave number of the

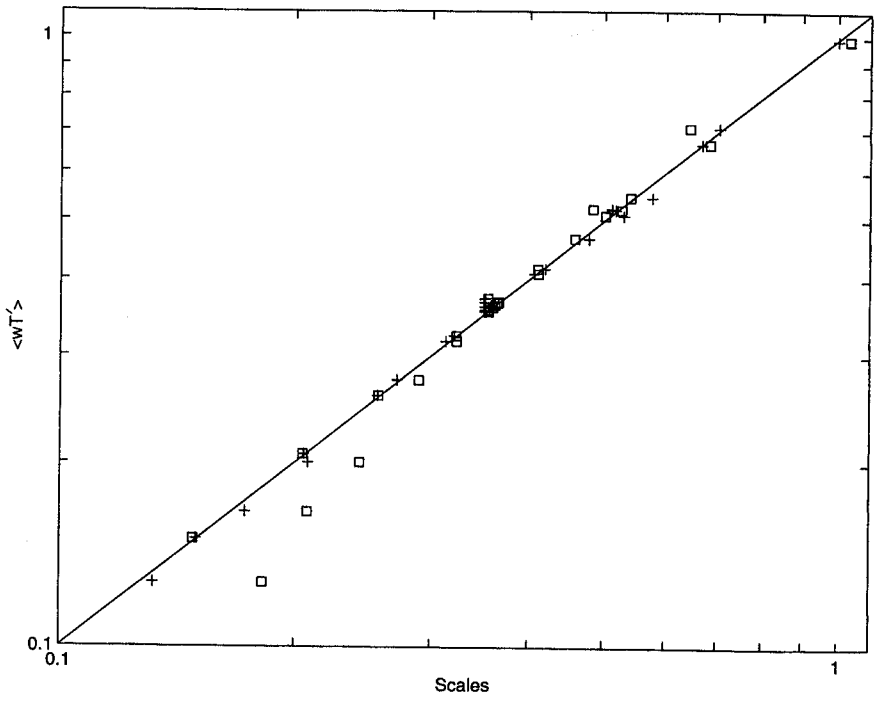

Figure 8. The domain-averaged convective heat flux, $\langle wT' \rangle$, versus the scale, Eq. (33), (+) with $c_1 = 0.333$ and its simpler variant in which the denominator in Eq. (33) is set to unity (□) and $c_1 = c_2 = 0.296$. The points plotted have moderate to small values of radiative, viscous, and diffusive damping. The scale, Eq. (33), fits the mean-field output better than the simpler variant, particularly at small $\langle wT' \rangle$. See text for further explanation.

most unstable mode. This keeps the aspect ratio of the convective cells approximately constant. When the other external parameters are varied, z_n does not vary strongly, and so a^2 is kept at the control-run value ($a^2 = 45.2$). This figure only plots points with moderate to small damping, that is, $\gamma \geqslant 7 \times 10^5$, $\kappa \leqslant 1/30$, and $r \leqslant 17$.

Figure 8 shows that the scaling, Eq. (33), has less scatter than its simpler variant. A least-squares fit of the coefficient c_1 in Eq. (33) yields $c_1 = 0.333 \pm 0.001$, whereas a least-squares fit for the coefficient $c_1 = c_2$ of the simpler scaling yields $c_2 = 0.296 \pm 0.0025$. The uncertainty of both parameter values is small, but the simpler scaling has a greater uncertainty than the more sophisticated scaling. However, an improved fit for the sophisticated scaling is expected, because this scaling has effectively two fitting coefficients — c_1, and the altitude at which α is evaluated — whereas the simpler scaling has only one fitting coefficient, c_2.

We have obtained scales for the correlation of w and T' (i.e. $\overline{wT'}^m$), but it is also of interest to develop individual scales for w and T'. To do so, we use mixing-length theory (e.g. Kraichnan 1962). We find a relationship between w and T' from the vertical component of the momentum equation (1). In the steady-state mean-field equations, the inertia terms vanish, leaving only the pressure-perturbation force, the buoyancy force, and the viscous force. Ignoring the pressure-perturbation force in the manner typical of mixing-length theory, we balance the viscous and buoyancy forces, as appropriate for a weakly nonlinear flow, to obtain

$$\frac{w}{z^2} = c_3 \gamma T', \tag{34}$$

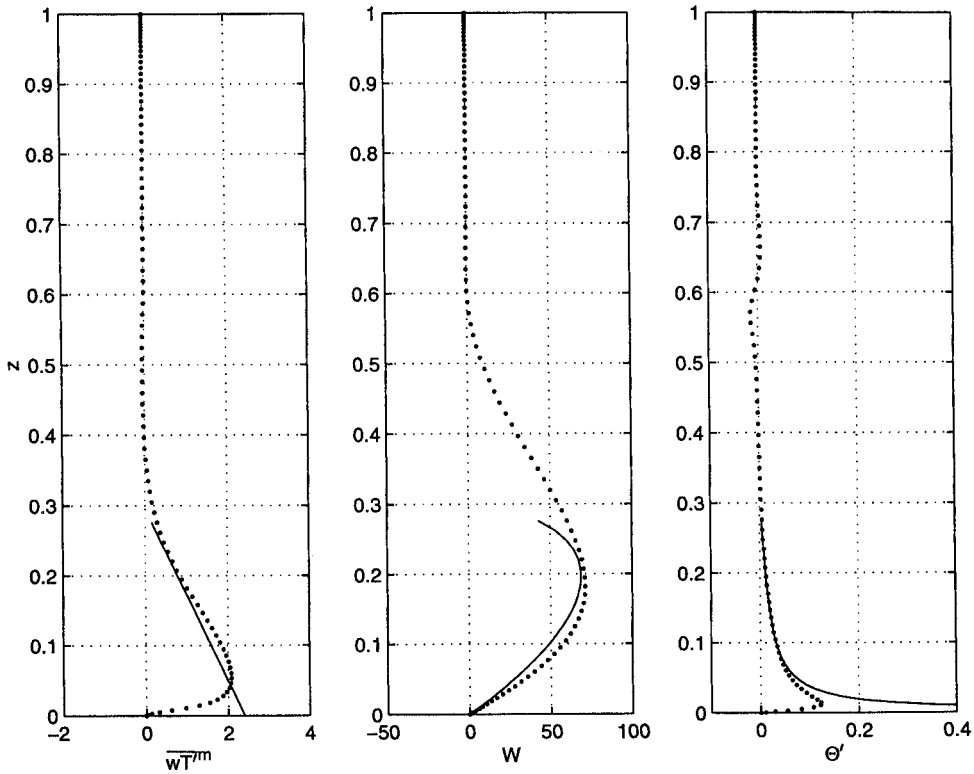

Figure 9. The control-run output from the mean-field equations (.), plus the scalings, Eq. (32), with denominator set to unity and $c_1 = c_2 = 0.296$, (37), and (38) for $\overline{wT'}^m$, $(\overline{w^2}^m)^{1/2}$, and $(\overline{T'^2}^m)^{1/2}$ (solid). In these equations, $c_3 = 0.217$. See text for further explanation.

where c_3 is a constant. Multiplying both sides of Eq. (34) by w, averaging over the horizontal, and taking the square root of both sides, we find a vertical-velocity scale:

$$(\overline{w^2}^m)^{1/2} = (c_3 \gamma \overline{wT'}^m)^{1/2} z \qquad \text{for} \qquad \overline{wT'}^m \geqslant 0. \tag{35}$$

Similarly, to find a temperature-perturbation scale, we multiply both sides of Eq. (34) by T', average horizontally, and take the square root of both sides:

$$(\overline{T'^2}^m)^{1/2} = \{\overline{wT'}^m/(c_3\gamma)\}^{1/2}\frac{1}{z} \qquad \text{for} \qquad \overline{wT'}^m \geqslant 0. \tag{36}$$

The scales, Eqs. (35) and (36), are not closed because they express w and T' in terms of $\overline{wT'}^m$. To obtain closed scales, we may substitute the simple scaling for $\overline{wT'}^m$ (Eq. (32) with the denominator set to unity and $c_1 = c_2$) into Eqs. (35) and (36), yielding, respectively:

$$(\overline{w^2}^m)^{1/2} = (c_3 \gamma c_2 F_T S)^{1/2}(z_n - z)^{1/2} z \qquad 0 < z < z_n \tag{37}$$

and

$$(\overline{T'^2}^m)^{1/2} = \left(\frac{c_2 F_T S}{c_3 \gamma}\right)^{1/2} \frac{(z_n - z)^{1/2}}{z} \qquad 0 < z < z_n. \tag{38}$$

These scales and the numerical output from the control run are displayed in Fig. 9, along with the simple scale for $\overline{wT'}^{m}$. The scales agree reasonably well with the numerical output in the mid troposphere. The fit turns out to be poorest for low S; in this case the maximum of the w scale occurs 1–2 km higher than in the numerical output (not shown).

Although the scales, Eqs. (37) and (38), adequately approximate the weakly nonlinear mean-field profiles for w and T' respectively, they would not be expected to describe the highly nonlinear convection characteristic of the atmosphere. The scales, Eqs. (37) and (38), assume a balance between buoyancy and viscous forces, whereas in atmospheric convection we expect a balance between buoyancy and inertia terms. With the latter balance, mixing-length theory then leads to the following relationship, written using dimensional quantities:

$$\frac{w_*^2}{z_*} \sim g_* \alpha_{T*} T'_*. \tag{39}$$

Assuming that w_* and T'_* are well correlated, we may obtain scales for w_* and T'_* in terms of $\overline{w_* T'_*}^{m}$:

$$w_* \sim (g_* \alpha_{T*} \overline{w_* T'_*}^{m} z_*)^{1/3} \qquad \text{for} \qquad \overline{w_* T'_*}^{m} \geqslant 0, \tag{40}$$

$$T'_* \sim \frac{(\overline{w_* T'_*}^{m})^{2/3}}{(g_* \alpha_{T*} z_*)^{1/3}} \qquad \text{for} \qquad \overline{w_* T'_*}^{m} \geqslant 0. \tag{41}$$

These scales are similar to those obtained by Prandtl (1932), Priestley (1959), and Deardorff (1970), except that here $\overline{w_* T'_*}^{m}$ is not a constant kinematic heat-flux scale, but a function of z_* determined largely by $\overline{F}_z^{m}$. Leaving $\overline{w_* T'_*}^{m}$ as a function of z_* leads to a more realistic prediction for w_* in the upper troposphere. When $\overline{w_* T'_*}^{m}$ is taken to be a constant, the w_* scale increases monotonically with increasing altitude. In a radiative–convective atmosphere, however, $\overline{w_* T'_*}^{m}$ is expected to become small near the tropopause and remain small in the stratosphere. Hence the expression, Eq. (40), for w_* would be expected to reach a maximum in the mid troposphere and decrease from there upwards. The scales, Eqs. (40) and (41), for w_* and T'_* have no explicit dependence on viscosity, as one might expect for strongly nonlinear atmospheric convection.

We may close the scales, Eqs. (40) and (41), via the simple scaling for $\overline{wT'}^{m}$ obtained by setting the denominator of Eq. (32) to unity. Although the scales, Eqs. (37) and (38), for the individual fields w and T' fail for strongly nonlinear flows, it is reasonable to suppose that the scale, Eq. (32), for $\overline{wT'}^{m}$ and its simpler variant are adequate for dry, strongly nonlinear, radiative–convective flows. In both weakly and strongly nonlinear flows, the convective heat flux is strongly constrained by the radiative flux, and the radiative flux, in turn, is constrained by the temperature profile. But even the weakly nonlinear flows that we have modelled here produce an adiabatic troposphere and a stratosphere in radiative equilibrium. This temperature profile is not likely to change in a strongly nonlinear flow. Therefore, we may expect that the $\overline{wT'}^{m}$ profile remains similar in weakly nonlinear and strongly nonlinear systems, even if the scalings of w and T' differ in the two systems. Rewriting the simple scale for $\overline{wT'}^{m}$ in terms of dimensional parameters and substituting it into Eqs. (40) and (41) yields, respectively,

$$w_* \sim \left(g_* \alpha_{T*} \frac{F_{T*}}{\rho_* c_{p*}} S_* (z_{n*} - z_*) z_* \right)^{1/3} \qquad 0 < z < z_n \tag{42}$$

and

$$T'_* \sim \left(\frac{F_{T*}}{\rho_* c_{p*}} S_*\right)^{2/3} \frac{1}{(g_* \alpha_{T*})^{1/3}} \frac{(z_{n*} - z_*)^{2/3}}{z_*^{1/3}} \qquad 0 < z < z_n. \tag{43}$$

The scale, Eq. (42), predicts that w_* has a single, broad maximum in the mid troposphere. Substituting reasonable numbers into Eqs. (42) and (43) yields $w_* \sim 3$ m s^{-1} and $T'_* \sim 0.1$ K at $z_* = 3$ km. Nearer to the ground, w_* is smaller and T'_* is larger. These values are orders of magnitude closer to atmospheric values than those that would be obtained from the scales, Eqs. (37) and (38).

9. Conclusions

The linear-stability properties of our radiative–convective model turn out to be similar to those of Rayleigh–Bénard convection. In both systems, instability arises as overturning cells rather than an oscillatory instability, and the mechanism of instability is similar. However, radiation does introduce two new effects: it causes thermal damping, and it largely determines the basic-state lapse rate. These effects can be incorporated into a stability analysis by constructing a radiative Rayleigh number. The effects of radiation on the stability can then be ascertained by inspection of this single parameter. Although the energy method can rule out the possibility of subcritical instability in Rayleigh–Bénard convection, it cannot do so for our radiative–convective model when radiative absorptivity varies with height, because then the radiative-equilibrium temperature profile is curved.

The radiative–convective and Rayleigh–Bénard systems differ fundamentally when weakly nonlinear convection occurs. Specifically, the damping parameters have only a weak effect on the convective heat flux in the radiative–convective model but a strong effect in the Rayleigh–Bénard system. The difference arises because of the strong constraints imposed by radiation. The damping parameters have a weak effect on convective heat flux in the radiative–convective model in part because convective heating must balance radiative cooling, and the radiative cooling, in turn, is strongly constrained by the requirements that the tropospheric lapse rate be adiabatic and that the stratosphere be in radiative equilibrium. Also important is the fact that it is the total heat flux at the top of the atmosphere, not the temperature, that is fixed by the net incoming solar radiation.

We have constructed dry radiative–convective scalings for buoyancy, velocity, and convective heat flux. Unlike the bulk buoyancy and velocity scales that have been proposed for moist systems, the dry scales predict the vertical variations of these quantities. The dry case is simpler because closed scales can be constructed from the momentum and heat equations alone. In the moist case, moisture effects contribute strongly to the heat equation, and closing the moisture terms is not trivial.

The result from our dry radiative–convective analyses that is most likely to carry over to a moist system is the result that the values of the damping parameters have little influence on convective heat flux. This result followed from simple and robust properties of the radiative flux and temperature profiles. However, it is possible that the values of the damping parameters may re-enter the moist problem if they significantly influence cloud cover or the water-vapour profile.

Acknowledgements

The author wishes to thank Kerry A. Emanuel, Richard M. Goody, W. V. R. Malkus, Glenn R. Flierl, R. Alan Plumb, Pablo Zurita, Gerard Roe, David Nolan, and two

anonymous referees for their insightful comments on this work. This research was supported by the US Department of Energy via Grant DE-FG02-91ER61220.

REFERENCES

Arpaci, V. S. and Gőzűm, D. 1973 Thermal stability of radiating fluids: The Bénard problem. *Phys. Fluids*, **16,** 581–588

Boyd, J. P. 1989 *Chebyshev and Fourier Spectral Methods*. Springer-Verlag, New York, USA

Castaing, B., Gunaratne, G., Heslot, F., Kadanoff, L., Libchaber, A., Thomae, S., Wu, X.-Z., Zaleski, S. and Zanetti, G. 1989 Scaling of hard thermal turbulence in Rayleigh-Bénard convection. *J. Fluid Mech.*, **204,** 1–30

Chan, S.-K. 1971 Infinite Prandtl Number turbulent convection. *Stud. Appl. Math.*, **50,** 13–49

Craig, G. C. 1996 Dimensional analysis of a convecting atmosphere in equilibrium with external forcing. *Q. J. R. Meteorol. Soc.*, **122,** 1963–1967

Davis, S. H. 1969 On the principle of exchange of stabilities. *Proc. R. Soc. London A*, **310,** 341–358

Deardorff, J. W. 1970 Convective velocity and temperature scales for the unstable planetary boundary layer and for Rayleigh convection. *J. Atmos. Sci.*, **27,** 1211–1213

Drazin, P. G. and Reid, W. H. 1981 *Hydrodynamic stability*. Cambridge University Press, New York, USA

Eady, E. T. 1949 Long waves and cyclone waves. *Tellus*, **1**(3), 33–52

Emanuel, K. A. 1994 *Atmospheric Convection*, Oxford University Press, New York, USA

Emanuel, K. A. and Bister, M. 1996 Moist convective velocity and buoyancy scales. *J. Atmos. Sci.*, **53,** 3276–3285

Goody, R. M. 1956 The influence of radiative transfer on cellular convection. *J. Fluid Mech.*, **1,** 424–435

1995 *Principles of atmospheric physics and chemistry*. Oxford University Press, New York, USA

Herring, J. R. 1963 Investigation of problems in thermal convection. *J. Atmos. Sci.*, **20,** 325–338

1964 Investigation of problems in thermal convection: Rigid boundaries. *J. Atmos. Sci.*, **21,** 277–290

Howard, L. N. 1963 Heat transport by turbulent convection. *J. Fluid Mech.*, **17,** 405–432

1964 'Convection at high Rayleigh number.' Pp. 1109–1115 in Proc. Eleventh Int. Congress Applied Mechanics, Munich. Springer-Verlag, Berlin, Germany

Joseph, D. D. 1965 Nonlinear stability of the Boussinesq equations by the method of energy. *Arch. Ration. Mech. Anal.*, **22,** 163–184

Kraichnan, R. H. 1962 Turbulent thermal convection at arbitrary Prandtl number. *Phys. Fluids*, **5,** 1374–1389

Larson, V. E. 1999a The effects of thermal radiation on dry convective instability. Submitted to *Dyn. Atmos. Oceans*

1999b The effects of thermal radiation on dry convection. PhD dissertation, Massachusetts Institute of Technology

Malkus, W. V. R. 1954 The heat transport and spectrum of thermal turbulence. *Proc. R. Soc. London A*, **225,** 196–212

Manabe, S. and Strickler, R. F. 1964 Thermal equilibrium of the atmosphere with a convective adjustment. *J. Atmos. Sci.*, **21,** 361–385

Murgai, M. P. and Khosla, P. K. 1962 A study of the combined effect of thermal radiative transfer and a magnetic field on the gravitational convection of an ionized fluid. *J. Fluid Mech.*, **14,** 433–451

Musman, S. 1968 Penetrative convection. *J. Fluid Mech.*, **31,** 343–360

Pellew, A. and Southwell, R. V. 1940 On maintained convective motion in a fluid heated from below. *Proc. R. Soc. London A*, **176,** 312–343

Pierrehumbert, R. T. 1995 Thermostats, radiator fins, and the local runaway greenhouse. *J. Atmos. Sci.*, **52,** 1784–1806

Prandtl, L. 1932 Meteorologische Anwendung der Strömungslehre. *Beitr. Phys. freien Atmosphäre*, **19,** 188–202

Press, W. H., Teukolsky, S. A., Vetterling, W. T. and Flannery, B. P. 1992 *Numerical recipes in C: The art of scientific computing. 2nd ed.* Cambridge University Press, New York, USA

Priestley, C. H. B. 1959 *Turbulent transfer in the lower atmosphere.* The University of Chicago Press, Chicago, USA

Rennó, N. O. and Ingersoll, A. P. 1996 Natural convection as a heat engine: a theory for CAPE. *J. Atmos. Sci.*, **53,** 572–585

Siggia, E. D. 1994 High Rayleigh number convection. *Annu. Rev. Fluid Mech.*, **26,** 137–168

Spiegel, E. A. 1960 The convective instability of a radiating fluid layer. *Astrophys. J.*, **132,** 716–728

1962 On the Malkus theory of turbulence. *Mécanique de la Turbulence*, Centre National de la Recherche Scientifique, Paris, France, 181–201

1971 Convection in stars I. Basic Boussinesq convection. *Annu. Rev. Astron. Astrophys.*, **9,** 323–352

Spiegel, E. A. and Veronis, G. 1960 On the Boussinesq approximation for a compressible fluid. *Astrophys. J.*, **131,** 442–447

Straughan, B. 1992 *The energy method, stability, and nonlinear convection.* Springer-Verlag, New York, USA

Stull, R. B. 1988 *An introduction to boundary layer meteorology.* Kluwer Academic Publishers, Dordrecht, the Netherlands

Sun, W.-Y. 1976 Linear stability of penetrative convection. *J. Atmos. Sci.*, **33,** 1911–1920

Tritton, D. J. 1988 *Physical fluid dynamics. 2nd ed.* Oxford University Press, New York, USA

Whitehead, J. A. and Chen, M. M. 1970 Thermal instability and convection of a thin fluid layer bounded by a stably stratified region. *J. Fluid Mech.*, **40,** 549–576